Self-Organized Criticality in Glassy Spin Systems Requires a Diverging Number of Neighbors

Juan Carlos Andresen,[1] Zheng Zhu,[2] Ruben S. Andrist,[1] Helmut G. Katzgraber,[2,1] V. Dobrosavljević,[3] and Gergely T. Zimanyi[4]

[1] *Theoretische Physik, ETH Zurich, CH-8093 Zurich, Switzerland*
[2] *Department of Physics and Astronomy, Texas A&M University, College Station, Texas 77843-4242, USA*
[3] *Department of Physics and National High Magnetic Field Laboratory, Florida State University, Tallahassee, Florida 32306, USA*
[4] *Department of Physics, University of California, Davis, California 95616, USA*

(Dated: May 29, 2018)

We investigate the conditions required for general spin systems with frustration and disorder to display self-organized criticality, a property which so far has been established only for the fully-connected infinite-range Sherrington-Kirkpatrick Ising spin-glass model [Phys. Rev. Lett. **83**, 1034 (1999)]. Here we study both avalanche and magnetization jump distributions triggered by an external magnetic field, as well as internal field distributions in the short-range Edwards-Anderson Ising spin glass for various space dimensions between 2 and 8, as well as the fixed-connectivity mean-field Viana-Bray model. Our numerical results, obtained on systems of unprecedented size, demonstrate that self-organized criticality is recovered only in the strict limit of a diverging number of neighbors, and is not a generic property of spin-glass models in finite space dimensions.

PACS numbers: 75.50.Lk, 75.40.Mg, 05.50.+q, 64.60.-i

Self-organized criticality (SOC) refers to the tendency of large dissipative systems to drive themselves into a scale-invariant critical state without any special parameter tuning [1, 2]. These phenomena are of crucial importance because fractal objects displaying SOC are found everywhere [3], e.g., in earthquakes, in the structure of dried-out rivers, in the meandering of sea coasts, or in the structure of galactic clusters. Understanding its origin, however, represents a major unresolved puzzle because in most equilibrium systems critical behavior featuring scale-free (fractal) patterns is found only at isolated critical points and is not a generic feature across phase diagrams.

Pioneering work in the 1980s provided insights into the possible origin of SOC by identifying a few theoretical examples that display it. The "sandpile" [4] and forest-fire models [5] are hallmark examples of dynamical systems that exhibit SOC. However, these models feature *ad hoc* dynamical rules, without showing how these can be obtained from an underlying Hamiltonian. Major questions thus remain: Can one obtain SOC from a Hamiltonian system, beyond invasion percolation [6, 7]? Is this behavior a feature of high-dimensional models, models with a diverging number of neighbors and/or long-range interactions, or is it a generic property of a broad class of systems?

Work in the 1990s offered a glint of hope. The first Hamiltonian model displaying SOC without any parameter tuning was studied in detail by Pazmandi *et al.* [8]: the infinite-range fully connected Sherrington-Kirkpatrick (SK) model [9]. Out-of-equilibrium avalanches at zero temperature ($T = 0$) triggered by varying the magnetic field were numerically studied along the hysteresis loop. A distinct power-law behavior in the distribution of spin avalanches, as well as of the magnetization jumps, was established, i.e., SOC.

The possible existence of SOC was also tested in several finite-dimensional models, but in all these cases, at least one parameter has to be tuned. The best-studied such model is the random-field Ising model where ferromagnetic Ising spins are coupled to a random field of average strength R. For space dimensions $d > 2$, a critical R_c exists where avalanches and magnetization jumps show SOC; i.e., the relevant distributions assume a power-law form [10–14]. Similar results were found for the random-bond Ising model [15], as well as the random-anisotropy Ising model [16], where by tuning a parameter SOC, can be observed.

A recent study [17] on the efficiency of hysteretic optimization [18] suggests that system-spanning avalanches might be favored in fully connected models. However, surprisingly, no numerical studies have been reported to date for the "vanilla" Edwards-Anderson Ising spin glass (EASG) [19] (Gaussian interactions with zero mean). Recently [20, 21], the possibility of SOC in the EASG for $d < \infty$ was suggested. The work is strictly valid at equilibrium (i.e., for switches in the ground state) and is based on droplet arguments (where a critical response is expected for fields close to zero). These results raise the question as to whether SOC might be present in out-of-equilibrium avalanche simulations of the EASG, as done for the SK model [8].

A deeper understanding of models that exhibit SOC is thus needed. Because the SK model is thought to be the mean-field limit of the EASG, standard lore would suggest that the EASG may display SOC for all space dimensions $d \geq 6$ (above the upper critical dimension $d_{\rm u}$ where mean-field behavior sets in). To understand whether mean-field behavior suffices or long-range interactions (with and without a diverging number of neighbors) are needed, we study field-driven avalanches at zero temperature for the EASG in $d = 2$ – 6, and 8 (with $z = 2d$ neighbors), as well as the Viana-Bray (VB) model ($d = \infty$, $z = 6$) [22]. In addition, we study spin glasses on scale-free graphs [23] where the number of neighbors is distributed according to a power law $\sim z^{-\lambda}$. Therefore, we probe the system below and above the (equilibrium) upper critical dimension, as well as for different combinations of interaction range and number of neighbors z. In addition, we compare to results for the SK model ($d = \infty$, $z = N - 1$, with N the number of spins). Our results demonstrate that as long as $d < \infty$, no SOC is present in the EASG. Furthermore, no SOC is present for the VB model ($d = \infty$ but $z = 6$ fixed) or spin glasses on scale-free graphs when the edge degree does not diverge with the system size ($\lambda > 2$). However, for the SK model, SOC is recovered. Our results therefore indicate that a diverging number of neighbors is the key ingredient to obtain SOC in glassy spin systems.

Model, Observables and Algorithm.— We study Ising models in d space dimensions with the Hamiltonian $\mathcal{H} = -\sum_{\langle i,j\rangle}^{N} J_{ij} S_i S_j - H\sum_i S_i$. Here $S_i = \pm 1$ represent $N = L^d$ Ising spins on hypercubic lattices of linear size L. The interactions J_{ij} are drawn from a Normal distribution with zero mean, and H represents a magnetic field that drives the avalanches. For $d = \infty$ (SK limit [9]), the sum is over all spins and the variance of the interactions is chosen as $1/(N-1)$. When $d < \infty$, the model is known as the nearest-neighbor EASG [19] where the interactions have variance 1. The VB model is similar to the SK model; however, the number of neighbors is fixed to 6. In the scale-free graphs, the distribution of z decays with a power law $\sim z^{-\lambda}$.

The algorithm used is zero-temperature Glauber dynamics [10, 12, 24]. We start by computing the local fields for all spins: $h_i = \sum_j J_{ij} S_j - H$. A spin is unstable if the stability $h_i S_i < 0$. The initial field H is selected such that $H > |h_i|$ $\forall i$. The spins are then sorted by h_i and the field H reduced until the stability of the first sorted spin crosses zero, making the spin unstable [25]. This unstable spin is flipped, then the local fields of the other spins are recalculated, and the most unstable spin is flipped again. The process is repeated until all spins become stable, i.e., their stabilities are non-negative. In most cases, the flipping of the first unstable spin triggers the flipping of a substantial number of other spins, therefore causing avalanches. The parameters are shown in Table I.

At each avalanche triggered by the above algorithm, we measure the number of spins n that flipped until the system regains equilibrium and record the distribution of avalanche sizes $D(n)$ for all triggered avalanches until $S_i \to -S_i$ $\forall i$. In addition, we measure the magnetization jump S at each avalanche and record the distribution of magnetization jumps $P(S)$ [26, 27]. For the SK model, the avalanches are expected to be power law distributed with an exponential cutoff that sets in at a characteristic size n^* (similar arguments are valid for the magnetization jumps with a characteristic size S^*). Only if $n^*(N) \to \infty$ as $N \to \infty$, does the system exhibit SOC. We determine n^* in two different ways: First, we fit the tail of the distributions to $D(n) \sim \exp\left[-n/n^*(N)\right]$ with $n^*(N)$ a parameter. We also fit the small-n regime to a power law and determine the point of closest proximity between the fits. This yields a second estimate of $n_{\rm c}^*(N)$ [see Fig. 1]. While $n^*(N)$ obtained by the two approaches can differ by as much as a factor of ~ 2, $n^*(N \to \infty)$ obtained by either definition exhibits the same qualitative behavior. We choose to fit the distributions and extract $n^*(N)$ for a given space dimension d and (linearly) extrapolate to $N = \infty$.

TABLE I: Simulation parameters: For each dimension d, we study $N = L^d$ spins ($d < \infty$) and average over $N_{\rm sa}$ disorder samples. For the SK, VB, and scale-free models ($d = \infty$), we study up to 32 000 spins with at least 15 000 disorder samples.

d	L	N	$N_{\rm sa}$
2	1000	1 000 000	15 000
2	2000	4 000 000	15 000
2	3000	9 000 000	14 880
2	4000	16 000 000	14 860
3	100	1 000 000	15 000
3	150	3 375 000	10 000
3	200	8 000 000	12 900
3	250	15 625 000	14 250
4	10	10 000	15 000
4	20	160 000	15 000
4	40	2 560 000	15 000
4	60	12 960 000	15 000
6	8	262 144	15 000
6	10	1 000 000	15 000
6	12	2 985 984	15 000
6	14	7 529 536	15 000
6	16	16 777 216	15 000
8	4	65 536	15 000
8	5	390 625	15 000
8	6	1 679 616	15 000
8	7	5 764 801	14 480
8	8	16 777 216	10 200

In addition, to study criticality for $H \sim 0$ in the short-range systems, we measure the avalanche distribution $D_0(n)$ and magnetization jump distribution $P_0(S)$ if and only if the field H crosses zero [see Figs. 2(c) and 2(d)]. These measurements are necessary for short-range systems because the existence of a spin-glass state in a field remains controversial [28–33]. Therefore, under this restriction, we expect to probe an actual (nonequilibrium) spin-glass state.

Reference [8] argued that a true SOC system suppresses avalanche formation and stabilizes itself by developing a power-law pseudogap in $P(h)$, the distribution of stabilities, similar to the Efros-Shklovski gap of the Coulomb glass. Requiring the system to be stable against avalanches gives stringent bounds on the exponent and the coefficient of the power-law form. Therefore, we also study the distribution of local fields (stabilities) $P(h)$ for h close to zero.

Results.— Figure 1 shows the avalanche size and magnetization jump distributions for the $d = 3$ EASG. Avalanches remains small; i.e., the cutoffs n^* and S^* do not scale with the system size. In fact, even though we simulate over 10^7 spins, the largest avalanches (which occur extremely rarely) are only of approximately 100 spins. A crossover from a power law to an exponential cutoff in the distributions occurs for rather small n and S, respectively, suggesting no SOC. The vertical dashed line in Fig. 1 corresponds to the extrapolated values of n^* and S^*, respectively.

Reference [8] reported that the SK model (the mean-field limit or formulation of the EASG) exhibits SOC. Therefore, one could expect that the EASG exhibits SOC above $d_{\rm u} = 6$. To test this expectation, we simulate systems in $d = 8$ dimensions [see Fig. 2]. Again, no visible power-law behavior is present, indicating that the system displays no SOC. To

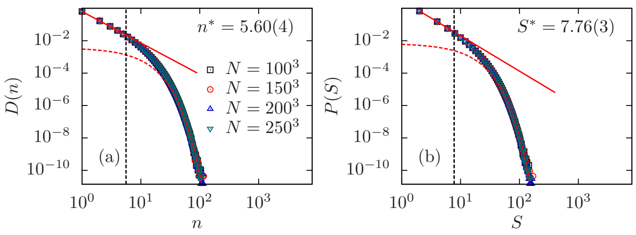

FIG. 1: (a) Avalanche distribution $D(n)$ for the $d = 3$ EASG. (b) Magnetization jump distribution $P(S)$. Both are recorded across the whole hysteresis loop and the data show no finite-size effects. The solid line represents a power law fit, whereas the dashed curve represents an exponential fit (see the text). The vertical dashed line marks the crossover value (n^* and S^* are determined by a fit to an exponential cutoff function; see the text).

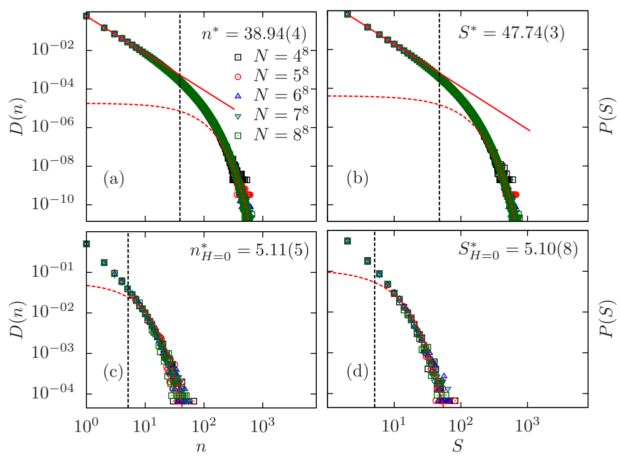

FIG. 2: (a) Avalanche distribution $D(n)$ for the $d = 8$ EASG. (b) Magnetization jump distribution $P(S)$. Both are recorded across the whole hysteresis loop. (c) Avalanche distribution $D_0(n)$ restricted to $H = 0$. (d) Magnetization jump distribution $P_0(S)$ restricted to $H = 0$. As in Fig. 1, the data show no finite-size effects. The solid line represents a power-law fit, whereas the dashed curve represents an exponential fit. The vertical (black) dashed lines mark the crossover value where a power law changes into an exponential. All panels have matching vertical and horizontal scales.

sidestep the debate over the existence of a spin-glass state in a field, we measure the avalanches only when H crosses zero, i.e., where it is most probable that the system is in a spin-glass state, even in a nonequilibrium type spin-glass state [26]. Because fluctuations are large when the restricted magnetization is measured, the data are noisy. However, again, no signs of SOC [see Figs. 2(c) and 2(d)].

Figure 3 shows data for the SK model. The data are in agreement with Ref. [8]: $D(n)$ [$P(S)$] has a power-law behavior for small n [S] with a crossover size $n^*(N)$ [$S^*(N)$] that diverges with N. A scaling collapse of the data agrees with the estimates of Ref. [8]. Furthermore, we find that $1/n^* = 0.00011(8)$ compatible with zero for $N \to \infty$, i.e., $n^* = \infty$. Data for the VB model (not shown) show no signs of SOC and are qualitatively similar to the data shown in Fig. 1. Data for spin glasses on scale-free graphs (not shown) only

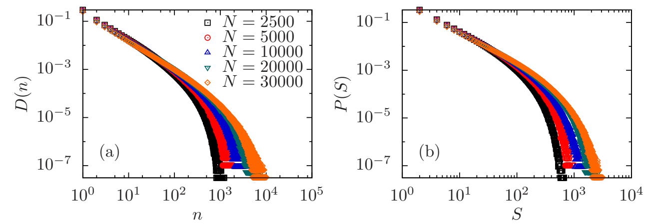

FIG. 3: (a) Avalanche distribution $D(n)$ for the SK model. (b) Magnetization jump distribution $P(S)$. Both are recorded across the whole hysteresis loop. The crossover from power law to an exponential cutoff behavior grows noticeably with N, signaling that the system displays SOC.

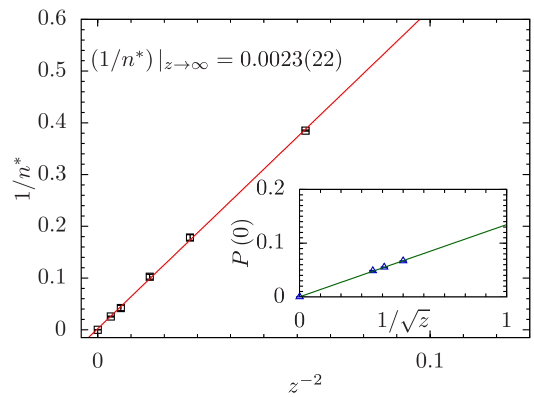

FIG. 4: (Color online) Inverse of the characteristic avalanche scale n^* as a function of coordination z. The data extrapolate perfectly to the SK limit, meaning that for *any* finite coordination number, the avalanches are finite in size for the EASG. The inset shows $P(h = 0)$ as a function of $z^{-1/2}$ for different space dimensions. $P(h = 0) = 0$ only for the SK model (data from Ref. [37]).

show a power-law behavior (i.e., SOC) when the number of neighbors diverges with the system size ($\lambda \leq 2$, Ref. [23]). Our results therefore show that a diverging number of neighbors (node degree) is a necessary condition for SOC to be present.

In Fig. 4, we plot the crossover avalanche size n^* as a function of the coordination $z = 2d$ and $d = 2 - 8$, as well as $z = \infty$ (SK). The data show that $n^* \propto z^2$; i.e., a true power-law behavior without a cutoff is only feasible for $z = \infty$ when the graph is complete [34]. Note that the same behavior is obtained for avalanches restricted to $H = 0$, as well as the magnetization jumps. Finally, our results are independent of the choice of n^* (either from a fit to an exponential or from the closest distance between the fitting function), illustrating the robustness of the effect. The inset of Fig. 4 shows $P(h = 0)$ as a function of the number of neighbors z. The data clearly show that $P(h = 0) \propto z^{-1/2} \to 0$ for $z \to \infty$ only; i.e., SOC is only present for the fully connected models, such as the SK model [35, 36].

Conclusions.— We have demonstrated that avalanches in short-range spin glasses do not span the system size, even if the space dimension d is above the upper critical dimension

$d_u = 6$. Our results suggest that SOC as found in Ref. [8] is not necessarily a property of the mean-field regime but is instead a result of a diverging number of neighbors z. Mean-field behavior can be reached in two equivalent ways, either by increasing d above d_u or by making the interactions infinite ranged ($z \to \infty$). Here, we show that these two limits can lead to different behaviors, which become equivalent only in the $d = \infty$ and of the infinite-range interaction limit. Analyzing models that allow for a continuous tuning of an effective space dimension [38–40] might thus also help in gaining further insights into this problem.

One has to keep in mind, however, that the conventional arguments [35] determining d_u are restricted to equilibrium states which below the glass transition temperature are typically difficult or impossible to reach experimentally. In contrast, the metastable states that the system visits on the outer hysteresis loop—which our avalanches explore—are indeed as far from equilibrium as possible. One should therefore not naively and indiscriminately apply equilibrium concepts such as the existence of the upper critical dimension $d_u = 6$ to the far-from-equilibrium behavior we study here. This might explain why we do not find critical system-spanning avalanches, as predicted in Refs. [20, 21] for static (equilibrium) response in short-range systems.

Our finding that the behavior of short-range models in any finite dimension remains fundamentally different than that of the fully connected infinite-range model is, therefore, a striking and a potentially far-reaching result. It calls for a change of perspective with respect to far-from-equilibrium states, and we hope that it will stimulate further efforts from the theoretical and the experimental community. The special role we suggest for the fully connected long-range interactions may have further interesting consequences, especially for bad metals near the metal-insulator transition [41]. Here, the Coulomb interaction between charge carriers assumes center stage, because poor screening in the bad metal regime directly reveals its long-range nature [42–44]. Existing work has already established that the single-particle density of states, which represents the direct analogue of $P(h)$ in this Letter, opens a power-law "Efros-Shklovskii" gap within the Coulomb glass phase [42–44]. Given our result that the vanishing of $P(0)$ is a direct manifestation of SOC, our findings strongly suggest that in the presence of frustrating fully connected long-range Coulomb interactions, SOC may survive [45, 46], even in physically-relevant space dimensions.

We would like to thank S. Boettcher, P. Le Doussal, M. Müller, and E. Vives for fruitful discussions. H.G.K. acknowledges support from the SNF (Grant No. PP002-114713) and the NSF (Grant No. DMR-1151387). V.D. was supported by the NSF (Grant No. DMR-1005751). We thank ETH Zurich for CPU time on the Brutus cluster.

[1] K. Schenk, B. Drossel, and F. Schwabl, in *Computational Statistical Physics*, edited by K. H. Hoffmann and M. Schreiber (Springer-Verlag, Berlin, 2002), p. 127.
[2] Note that within this context, SOC refers to criticality in zero-temperature field-driven disordered systems.
[3] B. B. Mandelbrot, *The Fractal Geometry of Nature* (Freedman, New York, 1983).
[4] P. Bak, C. Tang, and K. Wiesenfeld, Phys. Rev. Lett. **59**, 381 (1987).
[5] B. Drossel and F. Schwabl, Phys. Rev. Lett. **69**, 1629 (1992).
[6] C. M. Newman and D. L. Stein, Phys. Rev. Lett. **72**, 2286 (1994).
[7] M. Cieplak, A. Maritan, and J. R. Banavar, Phys. Rev. Lett. **72**, 2320 (1994).
[8] F. Pázmándi, G. Zaránd, and G. T. Zimányi, Phys. Rev. Lett. **83**, 1034 (1999).
[9] D. Sherrington and S. Kirkpatrick, Phys. Rev. Lett. **35**, 1792 (1975).
[10] J. P. Sethna, K. Dahmen, S. Kartha, J. A. Krumhansl, B. W. Roberts, and J. D. Shore, Phys. Rev. Lett. **70**, 3347 (1993).
[11] O. Perkovic, K. A. Dahmen, and J. P. Sethna, Phys. Rev. Lett. **75**, 4528 (1995).
[12] O. Perkovic, K. A. Dahmen, and J. P. Sethna, Phys. Rev. B **59**, 6106 (1999).
[13] M. C. Kuntz, O. Perkovic, K. A. Dahmen, B. W. Roberts, and J. P. Sethna (1998), (arXiv:cond-mat/9809122v2).
[14] J. P. Sethna, K. A. Dahmen, and O. Perkovic (2004), (arXiv:cond-mat/0406320v3).
[15] E. Vives and A. Planes, Phys. Rev. B **50**, 3839 (1994).
[16] E. Vives and A. Planes, Phys. Rev. B **63**, 134431 (2001).
[17] B. Gonçalves and S. Boettcher, J. Stat. Mech. P01003 (2008).
[18] K. F. Pal, Physica A **367**, 261 (2006).
[19] S. F. Edwards and P. W. Anderson, J. Phys. F: Met. Phys. **5**, 965 (1975).
[20] P. Le Doussal, M. Müller, and K. J. Wiese, Europhys. Lett. **91**, 57004 (2010).
[21] P. Le Doussal, M. Müller, and K. J. Wiese, Phys. Rev. B **85**, 214402 (2012).
[22] L. Viana and A. J. Bray, J. Phys. C **18**, 3037 (1985).
[23] H. G. Katzgraber, K. Janzen, and C. K. Thomas, Phys. Rev. E **86**, 031116 (2012).
[24] H. G. Katzgraber, F. Pázmándi, C. R. Pike, K. Liu, R. T. Scalettar, K. L. Verosub, and G. T. Zimányi, Phys. Rev. Lett. **89**, 257202 (2002).
[25] We use the "set" class contained in the standard C++ library to store and sort the spin stabilities (local fields). We thus take advantage of the optimized methods included in the standard library, enabling us to simulate systems with over 10^7 spins.
[26] In Ref. [8] the measurements are restricted to magnetization values in $[-0.3, 0.3]$ to improve statistics. In this work this restriction is not necessary because of the considerably larger system sizes studied, as well as much larger statistics. However, to perform a fair comparison, we have performed the simulations with the magnetization m restricted to $[-0.3, 0.3]$ obtaining qualitatively the same results.
[27] Note that there are small differences in the results obtained from the distribution of avalanche sizes $D(n)$ and the distribution of magnetization jumps $P(S)$ due to spin flips against the field direction because of the inherent frustration found in spin glasses. See also Ref. [8], where the obtained exponents for n and S differ for the same reason.

[28] J. R. L. de Almeida and D. J. Thouless, J. Phys. A **11**, 983 (1978).
[29] A. P. Young and H. G. Katzgraber, Phys. Rev. Lett. **93**, 207203 (2004).
[30] H. G. Katzgraber and A. P. Young, Phys. Rev. B **72**, 184416 (2005).
[31] T. Jörg, H. G. Katzgraber, and F. Krzakala, Phys. Rev. Lett. **100**, 197202 (2008).
[32] H. G. Katzgraber, D. Larson, and A. P. Young, Phys. Rev. Lett. **102**, 177205 (2009).
[33] R. A. Baños, A. Cruz, L. A. Fernandez, J. M. Gil-Narvion, A. Gordillo-Guerrero, M. Guidetti, D. Iñiguez, A. Maiorano, E. Marinari, V. Martin-Mayor, et al., Proc. Natl. Acad. Sci. U.S.A. **109**, 6452 (2012).
[34] We fit the data to $1/n^*(z) = 1/n^* + b/z^\gamma$. Allowing both $1/n^*$ and γ to vary, we obtain $1/n^* = -0.0015(23)$ and $\gamma = 1.91(4)$ with $Q = 0.99$ [47]. Fixing $\gamma = 2$, we obtain $1/n^* = 0.0023(22)$ with $Q = 0.99$. Fixing $1/n^* = 0$ and allowing γ to vary gives $\gamma = 1.93(3)$ with $Q = 0.99$. Therefore, the data are compatible with $1/n^* = 0$ and $\gamma \approx 2$.
[35] M. Mézard, G. Parisi, and M. A. Virasoro, *Spin Glass Theory and Beyond* (World Scientific, Singapore, 1987).
[36] P. R. Eastham, R. A. Blythe, A. J. Bray, and M. A. Moore, Phys. Rev. B **74**, 020406 (2006).
[37] S. Boettcher, H. G. Katzgraber, and D. Sherrington, J. Phys. A **41**, 324007 (2008).
[38] G. Kotliar, P. W. Anderson, and D. L. Stein, Phys. Rev. B **27**, 602 (1983).
[39] H. G. Katzgraber and A. P. Young, Phys. Rev. B **67**, 134410 (2003).
[40] L. Leuzzi, G. Parisi, F. Ricci-Tersenghi, and J. J. Ruiz-Lorenzo, Phys. Rev. Lett. **101**, 107203 (2008).
[41] V. Dobrosavljević, N. Trivedi, and J. M. Valles, *Conductor-Insulator Quantum Phase Transitions* (Oxford University Press, Oxford, England, 2012).
[42] M. Müller and L. B. Ioffe, Phys. Rev. Lett. **93**, 256403 (2004).
[43] S. Pankov and V. Dobrosavljević, Phys. Rev. Lett. **94**, 046402 (2005).
[44] M. Müller and S. Pankov, Phys. Rev. B **75**, 144201 (2007).
[45] A. A. Pastor and V. Dobrosavljević , Phys. Rev. Lett. **83**, 4642 (1999).
[46] A. A. Pastor, V. Dobrosavljević, and M. L. Horbach, Phys. Rev. B **66**, 014413 (2002).
[47] W. H. Press, S. A. Teukolsky, W. T. Vetterling, and B. P. Flannery, *Numerical Recipes in C* (Cambridge University Press, Cambridge, England, 1995).